On the Complexity of Routing and Spectrum Assignment in Flexible Grid Ring Networks

Massimo Tornatore, Cristina Rottondi, Roza Goscien,
Krzysztof Walkowiak, Giuseppe Rizzelli, and Annalisa Morea

I. Introduction

Today, fiber spectrum is typically divided using wavelength-division multiplexing (WDM) into separate channels with spacing of 50 GHz or 100 GHz. Optical signals are transmitted over each channel by transceivers supporting fixed line rates (e.g., 10, 40, or 100 Gb/s). As for the next generation of higher bit-rate transceivers (namely, at 400 Gb/s and 1 Tbps), they are expected not to fit the traditional grid at 50 or 100 GHz channel spacing due to insufficient inter-channel distance. Furthermore, innovative elastic transceiver architectures (capable of selecting their rates according to the network state by choosing the best combination among: modulation format, coding rate, and spectrum width) are being investigated. To exploit these elastic transceivers and to accommodate beyond-100 Gb/s rates, the conventional legacy grid has to evolve towards finer granularities, so that an arbitrary number of smaller frequency slices (e.g., 6.25 or 12.5 GHz [1]) can be used to create a channel serving the client demands with as much spectral resources as needed, provided that spectrum contiguity is ensured for all the slices belonging to the same channel (see Fig.1). Neighboring channels must be interleaved by guardbands to ensure proper filtering and switching, but such guardbands can be avoided/minimized in case of channels including multiple transceivers between the same source-destination node, forming a "superchannel". In short, while in the fixed grid each wavelength is switched individually, in flexible networks all the slices in the same channel are managed as a single entity [2]. Consequently, the Routing and Wavelength Assignment (RWA) traditionally solved for fixed grids has to evolve in a Routing and Spectrum Assignment (RSA) accounting for the additional spectrum adjacency and guardbands placement constraints.

It is well understood that introducing flexibility in the optical grid implies additional complexity in the network design and control plane. In addition, complexity further increases if we consider additional optimization dimensions such as: *traffic grooming* (i.e., how to groom multiple low-rate flows by means of electronic processing to aggregate larger traffic units to be mapped onto higher-capacity optical channels), the *assignment of different baud rates and modulation formats* to different transceivers in the network, and the *3R regeneration* in the optical layer. Intuitively, such additional dimensions increase the number of network configurations to be explored. However, we argue here that not in all network scenarios the advantages introduced by the above features are significant; e.g., a network scenario with several low-volume traffic requests would benefit more from grooming w.r.t. one with a few high-rate connections, or a network with short links would use less regeneration that a network with longer links.

This paper addresses the following questions: i) how much additional complexity is introduced in the RSA optimization by considering traffic grooming and/or regeneration and/or variable modulation formats and baud rates? ii) under which network and traffic conditions are the actual resource utilization savings worth the additional problem complexity? Complexity is evaluated in terms of i) number of variables and constraints of the ILP models, and ii) computational time required to obtain optimal network configurations. Resource utilization is expressed by the number of installed transceivers, N_t and by the overall spectrum occupation, S_o. To answer those question, we model and solve the RSA problem through Integer Linear Programming (ILP) formulations

M. Tornatore and C. Rottondi are with the Department of Electronics, Information, and Bioengineering, Politecnico di Milano, Italy (e-mail: {massimo.tornatore,cristinaemma.rottondi}@polimi.it).

G. Rizzelli is with Network Rail Telecom, Milton Keynes, UK (e-mail:giuseppe.rizzelli@networkrail.co.uk)

A. Morea is with Optical Networks Department, Alcatel-Lucent Bell Labs, Paris, France (e-mail:annalisa.morea@alcatel-lucent.com)

K. Walkowiak and R. Goscien are with the Faculty of Electronics, Department of Systems and Computer Networks, Wroclaw University of Technology, Poland (e-mail:{krzysztof.walkowiak,roza.goscien}@pwr.edu.pl)

in a wide range of ring network scenarios. Backbone and metro network (possibly interconnecting large data centers) represent today the main arena for the adoption of flexible-grid optical technologies. These network are typically ring-based or meshed with limited connectivity degree. Therefore, in order to limit the complexity of our approaches, in this study we focus only on the specific case of ring networks. We consider modeling the problem by adopting either a slice-based or channel-based approach: the former handles each slice individually, whereas the latter uses precomputed subsets of contiguous slices of different bandwidths. Note that these are two most common modeling approaches for the RSA problem [3], [4], but an exhaustive comparison of the two approaches has never been performed. Moreover, in the performance comparison we also include a benchmark model designed for the traditional WDM fixed grid, which can as well support traffic grooming, multiple baud rates/modulation formats and 3R regeneration, but uses the traditional 50 GHz spectrum granularity and does not support channel/superchannel formation, thus not requiring spectrum contiguity and guardband insertion constraints. Similar conclusions as those obtained in this study for ring networks are expected to yield for mesh network, but a more thorough investigation of this aspect is left for future investigation.

The rest of the paper is organized as follows. Section II provides a brief overview of the related work. Section III describes the flexigrid ring network architecture, whereas the details of the ILP formulations to solve the RSA problem are reported in Section IV. The complexity and the performance assessment of the proposed models are evaluated in Section V and VI, respectively. Section VII concludes the paper.

II. Related Work

The possible adoption of a flexible optical grid has stimulated a large number of studies in these last years (see [5] for a tutorial overview on physical layer technological and control plane aspects, as well as on network optimization approaches for flexible networks). In particular, the RSA problem has been widely studied and several exact models and heuristic approaches have been proposed (see Refs. [6]–[13]). The RSA problem has been proven to be NP-complete [3], even in case of chain and ring topologies [14], [15]. Ref. [14] also proposes approximated algorithms for binary trees and ring networks, and heuristic approaches for general mesh topologies. In Ref. [3], the complete Routing, Modulation Level and Spectrum Assignment RMLSA problem is investigated, considering that optical channels with different modulation formats can coexist; typically in RMLSA, the modulation is selected according to the traffic rates and channel length [16]. The ILP model propsosed in [3] uses a slice-based approach that we will employ also in this paper. Another model that explicitly accounts for the spectrum adjacency constraint in RSA is proposed in [8], but it does not account for multiple modulation formats. The authors of [4] propose and evaluate several ILP formulations of the RSA problem, including a channel-based one, where channel is defined as a precalculated set of adjacent frequency slices, such that the spectrum contiguity constraint is automatically satisfied. As we will demonstrate in the following Sections, this modeling approach is especially useful when the sets of traffic demands and routing paths are

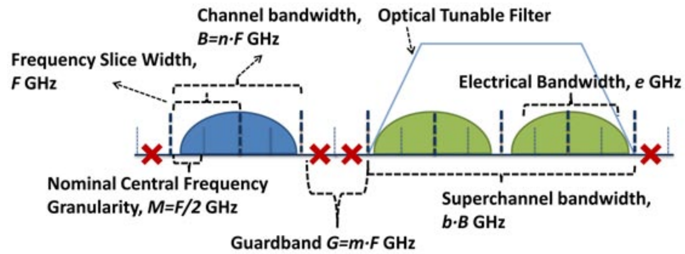

Fig. 1. Spectrum assignment with flexible grid

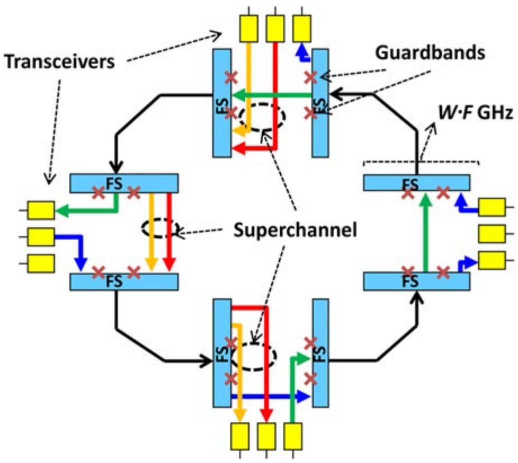

Fig. 2. The flexi-grid optical network (FS=Flexible-bandwidth optical switch)

given in advance. Ref. [17] formulates four link-based and route-based linear programs for the RSA problem in elastic networks and compares their complexity and applicability in terms of solving approach (e.g. usage of column generation or branch and price techniques), but no considerations are drawn on the effect of other optimization dimensions beyond the basic RSA (e.g, regeneration, or grooming traffic, as in this paper). RSA with regeneration in flexible networks is also a quite recent topic [18], [19] but some preliminary works are appearing. E.g., Ref. [19] proposes an effective placement of regenerators that allows to obtain substantial gain of network capacity. Ref. [20] considers ILP models and heuristics for time-varying traffic scenarios. In this paper, we provide two main novel contributions with respect to existing studies: 1) we explore the trade-off between network cost and problem complexity under multiple assumptions in terms of traffic grooming, regeneration, modulation/baud rate assignment capabilities; 2) we compare the performance of two alternative models: the slice-based model vs. the channel-based model.

III. Network Architecture and Assumptions

Topology. We consider a ring physical topology with a radius of R km, N nodes, and $E = 2N$ optical links, deployed in both clockwise and counterclockwise directions between each pair of contiguous nodes (see Fig. 2). Nodes are equipped with Flexible bandwidth optical switches.

Spectrum. We assume the optical spectrum to be partitioned in a grid of frequency slices of width FGHz ("granularity F GHz") as depicted in Fig. 1. The nominal central frequency M is placed in the middle of the slice, which imposes

TABLE I
REACH VALUES FOR VARIOUS MODULATION FORMATS (KM) AND FOR 28 GBAUD AND 14 GBAUD TRANSCEIVERS

h(GHz)	B (GHz)	h/B	QPSK	8-QAM	16-QAM	32-QAM	64-QAM
28 (14)	31,25 (18,75)	≈ 0.9 (≈ 0.75)	3050 (6300)	1010 (2100)	495 (1100)	198 (400)	138 (280)
28	50	0.56	3500	1400	630	220	150

that optical carriers used to transmit the optical signals are placed at predefined frequencies, which are regularly spaced along the spectrum every $M = F/2$ GHz, as mandated in [1]. The total spectrum width available on each optical link is $S = kF$ GHz, where k is an integer number.

Transceivers. We consider coherent transceivers, that apply Digital Signal Processing (DSP) techniques for compensation of transmission distortion, such as chromatic and polarization mode dispersion, and support advanced modulation formats, ie., different possible bit rates. Such transceivers have an electrical bandwidth of e GHz and operate at fixed baud rate of $h = h_{net} + h_{fec}$ GBaud, where h_{net} indicates the amount of net transmitted symbols per second and h_{fec} accounts for the redundant error coding. Given the spectral efficiency η (bit/s/Hz) of the modulation format in use (i.e., the net bit rate per Hertz), the transceiver capacity can be computed as ηh_{net}. The channel bandwidth B (GHz) indicates the width of the spectrum portion that has to be assigned to the optical signal generated by the transceiver, i.e., the bandwidth of the optical filter used to multiplex the signal[1]. To adapt to the granularity of the flexible grid, the channel bandwidth must be an integer multiple of the slice width F (i.e., it must hold that $B = nF$ and $B > e$). Since $M = F/2$, n can be either odd or even. Note that the performance of the transceiver highly depends on the choice of n: a high h/B ratio allows for high spectrum utilization, but decreases signal reach, i.e, the distance that can be covered without electronically regeneration of the signal. The reduction in reach is mainly caused by additional crosstalk due to adjacent channel coherent interference, and is more pronounced with advanced modulation formats. Table I reports the maximum reaches for different modulation formats and various combinations of the baud rates and optical bandwidths used in this work. Reaches have been computed based on the results in [21].

Superchannel. In case of low traffic volumes, multiple low-rate flows can be electronically groomed in the capacity of a single transceiver. In case the volume of traffic requests exceeds the maximum capacity that a transceiver can support, traffic demands can be served by transmitting the signals using multiple transceivers. In this case, a channel obtained by placing contiguously multiple transceivers is called superchannel and is handled by the optical switching equipment as a single entity, provided that each (super)channel is separated from the adjacent channels by a guard band $G = mF$ (GHz) (Fig. 1). Such frequency band between neighboring channels prevents overlapping and crosstalk among modulated signals. Note that the superchannel bandwidth, can be computed as bB, where b is the number of transceivers used to serve the traffic request.

IV. THE RSA PROBLEM

The RSA problem consists in assigning to each flow an optical path connecting the source and destination nodes and in allocating a portion of spectrum on each link traversed by the path. The basic RSA has been extended to cover additional design dimensions: in our previous work [22], based on the model presented in [23], we proposed ILP formulations jointly considering traffic grooming, the choice of the modulation format to be assigned to each optical channel, and of the baud rate of every transmitting unit. Here, we also include the regeneration capabilities (the "translucent" RSA problem) with 3R regenerators at the optical layer installed at intermediate nodes to increase the transmission reach For both the fixed and flexible grid, we exploit ILP models under four different RSA problem settings: the first is the traditional RSA problem, which considers neither traffic grooming[2] nor regeneration at the optical layer; the second considers grooming (RSA-G); the third regeneration (RSA-R); the fourth both grooming and regeneration (RSA-RG). For each setting, we explore four variants according to the transceiver characteristics (in terms of "elasticity"), i.e., fixed (Fx), variable modulation format (Mf), variable baud rate (Br) or variable modulation format and baud rate (Mf-Br). Therefore, the total number of explored problem settings is 16, and for each of them we consider different network topologies and traffic matrices (see Figure 3).

VARIABLE MOD. FORMAT \ VARIABLE BAUD RATE	YES			NO		
	REGEN. \ GROOM.	YES	NO	REGEN. \ GROOM.	YES	NO
YES	YES	RSA-RG Mf-Br	RSA-R F Mf-Br	YES	RSA-RG Mf	RSA-R F Mf
	NO	RSA-G Mf-Br	RSA Mf-Br	NO	RSA-G Mf	RSA Mf
	REGEN. \ GROOM.	YES	NO	REGEN. \ GROOM.	YES	NO
NO	YES	RSA-RG Br	RSA-R F Br	YES	RSA-RG Fx	RSA-R Fx
	NO	RSA-G Br	RSA Br	NO	RSA-G Fx	RSA Fx

Fig. 3. The considered network settings.

We now start describing the ILP model for the RSA-RG setting supporting both multiple transceiver baud rates and modulation formats (Mf-Br). i.e., the most comprehensive case. Then we discuss how to adapt/downgrade the model to the other simpler settings.

[1]Note that the channel bandwidth is usually wider than the electrical bandwidth.

Objective Function

$$\min \alpha_1 \sum_{i,j\in N,k\in K,h\in H,z\in Z:i\neq j} (2b^{hz}_{ijk} + \Gamma z b^{hz}_{ijk}) + \alpha_2 \sum_{i,j\in N,k\in K:i\neq j} L_{ijk}(\sum_{h\in H,z\in Z} b^{hz}_{ijk}F_h + y_{ijk}G) \tag{1}$$

Constraints

$$\sum_{k\in K} x^{sd}_{ijk} \leq 1 \qquad \forall i,j,s,d\in N: i\neq j, s\neq d \tag{2}$$

$$\sum_{\substack{s\in N,\\ d\in N:s\neq d}} x^{sd}_{ijk}t^{sd} \leq \sum_{\substack{h\in H,\\ z\in Z}} r^{hz}_{ijk}C_h b^{hz}_{ijk} \quad \forall i,j\in N, k\in K: i\neq j \tag{3}$$

$$x^{sd}_{ijk} \leq y_{ijk} \qquad \forall i,j,s,d\in N, k\in K: i\neq j, s\neq d \tag{4}$$

$$f_{ijk} + \sum_{\substack{h\in H,\\ z\in Z}} b^{hz}_{ijk}F_h + G \leq S \qquad \forall i,j\in N, k\in K: i\neq j \tag{5}$$

$$\sum_{k\in K, j\in N: i\neq j} x^{sd}_{ijk} - \sum_{k\in K, j\in N: i\neq j} x^{sd}_{jik} = \begin{cases} 1 \text{ if } s=i \\ -1 \text{ if } d=i \\ 0 \text{ otherwise}\end{cases} \qquad \forall i,s,d\in N: s\neq d \wedge t^{sd}>0 \tag{6}$$

$$(f_{i'j'k'} - f_{ijk}) \leq S d_{ijki'j'k'} \qquad \forall i,j,i',j'\in N, k,k'\in K: E_k(ij)\cap E_{k'}(i'j')\neq\varnothing \tag{7}$$

$$(f_{ijk} - f_{i'j'k'}) \leq S d_{i'j'k'ijk} \qquad \forall i,j,i',j'\in N, k,k'\in K: E_k(ij)\cap E_{k'}(i'j')\neq\varnothing \tag{8}$$

$$d_{ijk,i'j'k'} + d_{i'j'k'ijk} = 1 \qquad \forall i,j,i',j'\in N, k,k'\in K: E_k(ij)\cap E_{k'}(i'j')\neq\varnothing \tag{9}$$

$$f_{ijk} + \sum_{\substack{h\in H,\\ z\in Z}} b^{hz}_{ijk}F_h + G - f_{i'j'k'} \leq (S+G)(1-d_{i'j'k'ijk}+2-y_{ijk}-y_{i'j'k'}) \quad \forall i,j,i',j'\in N, k,k'\in K: E_k(ij)\cap E_{k'}(i'j')\neq\varnothing \tag{10}$$

$$f_{i'j'k'} + \sum_{\substack{h\in H,\\ z\in Z}} b^{hz}_{i'j'k'}F_h + G - f_{ijk} \leq (S+G)(1-d_{ijki'j'k'}+2-y_{ijk}-y_{i'j'k'}) \quad \forall i,j,i',j'\in N, k,k'\in K: E_k(ij)\cap E_{k'}(i'j')\neq\varnothing \tag{11}$$

A. RSA-RG *Slice-based Integer Linear Programming Formulation*

Parameters:

- N: set of nodes of the ring network
- L: set of physical links (m,n) of the ring network
- $K = \{1,2\}$: set of directions (1=clockwise, 2=counter-clockwise)
- H: set of possible transceiver baud rates
- F: spectral width of a frequency slice
- F_h: optical bandwidth of transceiver with baud rate h, expressed as integer multiple of F
- $Z = \{0,\ldots,|N|-2\}$: set of possible cardinalities of the set of regenerators placed along a lightpath
- S: total available spectrum width on each link[3].
- G: width of the guardband (GHz) used to separate adjacent spectrum paths, expressed as integer multiple of F
- r^{hz}_{ijk}: Spectral Efficiency (SE) along the lightpath between node i and node j in direction k using transceivers with optical bandwidth h and z regenerators (expressed as multiple of the basic SE of BPSK and computed according to the lightpath length and the reach limitations of the various modulation formats)
- C_h: capacity of a transceiver with baud rate h associated to the BPSK modulation format (Gb/s)
- $T^{sd} = \{t^{sd}\}$: traffic matrix between source-destination pairs (Gb/s)
- L_{ijk}: number of links traversed by the lightpath between node i and node j in direction k
- $E_k(ij)$: set of physical links traversed by lightpath (i,j) in direction k (if established)
- Γ: regenerator cost to transceiver cost ratio

Variables:

- x^{sd}_{ijk}: boolean variable, indicates whether a lightpath established between (i,j) node pair in direction k is used to serve the connection request between (s,d)
- b^{hz}_{ijk}: integer variable, indicates the number of transceiver pairs with baud rate h used to serve the lightpath between (i,j) node pair in direction k with z regenerators
- y_{ijk}: boolean variable, is 1 if a lightpath is established between (i,j) node pair in direction k
- f_{ijk}: positive variable, indicates the starting frequency of the lightpath between (i,j) node pair in direction k
- $d_{ijki'j'k'}$: boolean variable, is 0 if $f_{i'j'k'} < f_{ijk}$, 1 otherwise

Objective function: By varying the parameters α_1 and α_2, the objective function (1) allows minimizing either *i*) the number of transceivers and regenerators to be installed (in case $\alpha_1 \gg \alpha_2$) or *ii*) the overall spectrum occupation (in case $\alpha_1 \ll \alpha_2$). Note that in case *i*) if we assign a small positive value to α_2, the model will still minimize the number of installed transceivers but in case of multiple solutions, the model will choose the one that occupies the lowest amount of optical spectrum. Similar considerations hold for case *ii*), in which in case multiple configurations minimizing the spectrum occupation exist, the one requiring the lowest amount of transceivers/regenerators is selected. Note also that the parameter Γ defines the regenerator-to-transceiver normalized cost, which depends on the technological characteristics of the devices.

Constraints: Constraint (2) ensures that no bifurcation of traffic flows occurs by imposing that each traffic request is routed along a single direction (either clockwise or counter-clockwise, as this formulation is for a ring topology), while

[2]Please note that whenever traffic grooming is performed in electronic layers (RSA-G), also regeneration occurs at the electronic layer, but in our RSA-RG approach we consider in addition the possibility to perform regeneration at the optical layer.

[3]Note that in this paper we set S to values which ensure that the blocking probability is null, meaning that optical resources are always sufficient to serve all the traffic requests.

Constraint (4) imposes coherence of the values of y_{ijk} and x_{ijk}^{sd} variables by forcing the lightpath indicator y_{ijk} to be 1 if the lightpath (i,j) in direction k is used to serve at least one traffic request. Flow conservation is imposed by Constraint (6), while Equation (3) considers the capacity constraints and allows the possible grooming of traffic requests sharing the same lightpath. More in detail, the constraint computes the number of transceivers required to support all the traffic groomed along lightpath (i,j) in direction k according to the lightpath length: if intermediate regenerators are placed along the lightpath, the lightpath is split in multiple consecutive shorter fragments, which allows for the usage of more advanced modulation formats characterized by shorter reaches and in turn increases the capacity of the transceivers. Moreover, the choice of the transceiver baud rate also influences the transmission capacity. The correct ordering of the starting frequencies of the lightpaths having at least one common link is guaranteed by Equations (7), (8) and (9) by ensuring that either $f_{ijk} < f_{i'j'k'}$ or $f_{ijk} > f_{i'j'k'}$. Moreover, the starting frequencies are forced to assume a value in the available range of spectrum by Constraint (5). The correct placement of the guardbands between adjacent optical (super)channels is imposed by Constraints (10) and (11): these are activated only in case y_{ijk} and $y_{i'j'k'}$ are both set to 1 and are mutually exclusive, depending on the value of $d_{ijki'j'k'}$. In particular, when Constraint (10) is activated, it becomes $(f_{ijk} + b_{ijk})F + G < f_{i'j'k'}F$, thus ensuring that the frequency slices allocated for the two lightpaths (i,j,k) and (i',j',k') do not overlap. Similar considerations can be drawn for Constraint (11).

1) RSA-G *Slice-based Adaptation:* The model provided in Section IV-A can be reduced to RSA-G by setting $Z = \{0\}$ and maintaining variables and constraints unaltered.

2) RSA-R *Slice-based Adaptation:* Grooming can be eliminated by suppressing variable x_{ijk}^{sd} and Constraints (2), (3), (4). Moreover, Constraint (6) must be replaced by the following equation:

$$\sum_{k\in K} y_{ijk} = \begin{cases} 1 \text{ if } T^{ij} > 0 \\ 0 \text{ otherwise} \end{cases} \qquad \forall i,j \in N \qquad (12)$$

Note also that the usage of a single transceiver baud rate can be imposed by defining H as a singleton set, while the usage of single/multiple modulation formats can be completely captured by properly defining the capacity multiplier r_{ijk}^{sd} as in [3].

B. RSA-RG *Channel-based Integer Linear Programming Formulation*

In this subsection, we formulate the RSA-RG problem using a channel-based approach [4]. As mentioned above, in flexi-grid networks the spectrum is divided in frequency slices of the same size F, which we denoted here as $[a_1, a_2, \ldots, a_S]$ where S is the total number of slices available on each link. A *channel* is defined as a set of contiguous (adjacent) slices. In more detail, if a lightpath needs exactly n slices the possible channels for allocation of spectrum for this lightpath are $[a_1, a_2, \ldots, a_n]$, $[a_2, a_3, \ldots, a_{n+1}]$, …, $[a_{S-n+1}, a_2, \ldots, a_S]$. The main motivation behind the channel approach is to enable easy control of the spectrum overlapping in flexi-grid networks. Let C denote a set of all defined channels. Each channel $c \in C$ is described by a constant n_c, denoting the number of contiguous slices in channel c, and constant γ_{ca}, that is 1 if channel c uses slice a, and 0 otherwise. In the optimization, the channel for each lightpath is selected according to a binary variable y_{ijkc} that is 1, if channel c is used to realize lightpath (i,j) in direction k and 0 otherwise. Values of y_{ijkc} enable also controlling the slice overlapping. In particular, the term $\sum_{i,j\in N,k\in K,c\in C:i\neq j} \gamma_{ca}\delta_{ijkl}y_{ijkc}$ can be used to check how many lightpaths use slice a in link l, where the binary constant δ_{ijkl} determines whether link l belongs to a path realizing lightpath (i,j) in direction k. To avoid overlapping of slices, this term cannot exceed 1.

Parameters (additional):

- δ_{ijkl}: it is 1 if link l belongs to lightpath (i,j) in direction k; 0, otherwise
- A: set of slices available in the network
- C: set of channels, each channel contains a set of contiguous slices
- n_c: number of contiguous slices in channel c
- γ_{ca}: it is 1 if channel c uses slice a; 0, otherwise

Variables (additional):

- $y_{ijkc} = 1$: if channel c is used for lightpath (i,j) in direction k, 0 otherwise

Objective function: Equation (13) is very similar to (1), however the spectrum occupation (the second term) is defined according to the channel approach, i.e., $y_{ijkc}n_c$ provides the number of spectrum slices allocated to provision lightpath (i,j) in direction k using channel c.

Constraints: Equations (2), (3) and (6) are the same as in the previous model. Constraint (14) is introduced in the model to ensure that at most one spectrum channel is used for a lightpath (i,j) in direction k. Constraint (15) imposes coherence of the values of y_{ijkc} and x_{sdijk} variables by forcing the lightpath indicator y_{ijkc} to be 1 if the lightpath (i,j) in direction k is used to serve at least one traffic request. To assure that a channel selected for a lightpath (i,j) in direction k provides enough slices in the network we use constraint (16). In more detail, the left-hand side of (16) is equal to number of slices required by the transceivers $\sum_{h\in H,z\in Z} b_{ijkhz}F_h$. The right-hand side is equal to the number of slices provided by channel c selected for a lightpath (i,j) in direction k minus G slices for the guardband. To guarantee that a slice on a particular link can be allocated to at most one lightpath, i.e., the slices are not overlapped in the network, we add to the model Constraint (17).

Similarly to the previous model, also in this case the channel-based RSA-RG can be adapted to solve RSA-G and RSA-R. In more detail, the channel-based model can be reduced to RSA-G by setting $Z = \{0\}$ and keeping all variables and constraints unaltered. In the case of the RSA-R version of the model, we must consider two cases. First, we assume that variable baud rate (Br) is used. Therefore, the number of transceivers required between node i and node j, and consequently the number of spectrum slices required between these nodes is not constant, due to the variable b_{ijk}^{hz}. Therefore, channels $c \in C$ that can be selected for node pair (i,j) must be of various size n_c, which significantly increases the number of channels to be considered in the model for each node pair. To obtain RSA-R, we must remove from the RSA-RG model variable x_{ijk}^{sd} and Constraints (2), (3), (6). Moreover, we must replace Constraint (14) with:

$$\sum_{k\in K,c\in C} y_{ijkc} = \begin{cases} 1 \text{ if } T^{ij} > 0 \\ 0 \text{ otherwise} \end{cases} \qquad \forall i,j \in N \qquad (18)$$

Objective Function

$$\min \alpha_1 \sum_{i,j \in N, k \in K, h \in H, z \in Z: i \neq j} (2b_{ijk}^{hz} + \Gamma z b_{ijk}^{hz}) + \alpha_2 \sum_{i,j \in N, k \in K: i \neq j} L_{ijk} F y_{ijkc} n_c \tag{13}$$

Constraints (2), (3), (6) and

$$\sum_{c \in C} y_{ijkc} \leq 1 \quad \forall i,j \in N, k \in K : i \neq j \tag{14}$$

$$x_{ijksd} \leq \sum_{c \in C} y_{ijkc} \quad \forall i,j,s,d \in N, k \in K : i \neq j, s \neq d \tag{15}$$

$$\sum_{h \in H, z \in Z} b_{ijkhz} F_h \leq \sum_{c \in C} (n_c - G) y_{ijkc} \quad \forall i,j \in N, k \in K : i \neq j \tag{16}$$

$$\sum_{i,j \in N, k \in K, c \in C: i \neq j} \gamma_{ca} \delta_{ijkl} y_{ijkc} \leq 1 \quad \forall l \in L, a \in A \tag{17}$$

In the second case of RSA-R we assume that a single transceiver baud rate is used. Then, we know exactly the spectrum requirement for lightpath (i,j) in direction k, due to the number of used transceivers calculated according to values of r_{ijk}^{hz}. Therefore, we can limit the candidate channels for lightpath (i,j) in direction k only to those that provide the number of slices required for a particular lightpath (i,j) in direction k. Let $C(i,j,k)$ denote a set of channels for lightpath (i,j) in direction k providing the requested number of slices. Using this notation, we can replace constraints (14) and (17), with:

$$\sum_{k \in K, c \in C(i,j,k)} y_{ijkc} = \begin{cases} 1 \text{ if } T^{ij} > 0 \\ 0 \text{ otherwise} \end{cases} \quad \forall i,j \in N \tag{19}$$

$$\sum_{i,j \in N, k \in K, c \in C(i,j,k): i \neq j} \gamma_{ca} \delta_{ijkl} y_{ijkc} \leq 1 \quad \forall l \in L, a \in A \tag{20}$$

V. Complexity Evaluation

We now compare the complexity of the two models described in Section IV in terms of number of variables and constraints. The comparison benchmark is the complexity of the model proposed in [24] to solve the classical Routing and Wavelength Assignment (RWA) problem in a fixed-grid ring network. Table II reports the number of variables and constraints of the ILP formulations for each setting in case of slice-based modeling: the models related to flexible grid exhibit a $O(N^4)$ dependency on the number of variables and constraints, while the complexity of the fixed-grid models varies from $O(WN^2)$ to $O(N^4)$. The introduction of multiple modulations impacts only on the values of the parameter r_{ijk}^{sd} and does not increase the problem complexity. Conversely, the usage of multiple baud rates and regeneration increase the number of variables, adding a term H and N, respectively, to the cardinality of the main variables modeling N_t. Finally, introducing traffic grooming impacts both on the number of variables and constraints: variables x_{ijk}^{hz} indicating the amount of traffic groomed along every lightpath due to each request must be included, and the corresponding flow conservation constraints must be added.

Table III shows the number of variables and constraints of the channel-based model, for both fixed and flexi-grid, with two cases in terms of the channel generation: all feasible channels and only selected channels. The former case assumes that for each lightpath we generate all feasible channels providing the required number of slices. This results in $\propto S$ possible channels for the Fx/Mf without grooming case, since in the case without grooming we can easily identify a limited set of channels with fixed width. To illustrate this issue we consider the following example. Let n denote the number of slices required for the demand. Since the slice requirement of the demand is fixed, there are $S-n+1$ possible channels providing n contiguous slices, namely $[a_1, a_2, \ldots, a_n]$, $[a_2, a_3, \ldots, a_{n+1}]$, $\ldots$, $[a_{S-n+1}, a_2, \ldots, a_S]$. If $n \ll S$, the number of possible channels can be estimated as $\propto S$. In all other cases, channels must be of various size (due to grooming and/or using variable baud rate) and consequently, the set of all feasible channels include $\propto S^2$ channels. This estimation follows from the fact that we must consider channels having size of 2, 3,..., S slices, and the number of these channels is $S-1$, $S-2$,...,1, respectively, resulting in a total number of available channels approximately $\propto S^2$. However, to reduce complexity of the model, we can limit the number of spectrum channels to some arbitrary selected value A, as shown in the last columns of Table III. If all feasible channels are allowed, the size of the models in terms of the variables depends on the number of nodes and number of slices (from $O(N^2S)$ to $O(N^4+N^2S^2)$) while the number of constraints depends additionally on the number of links and varies from $O(N^2+LS)$ to $O(N^4+LS^2)$. When only selected channels are used, the complexity of the models is similar, however in all cases S (or S^2) is replaced by A. Note that the introduction of additional constraints increases the complexity similarly to Table II. Comparing Table II to Table III, we can notice that comparison between slice-based model and channel-based model in terms of the number of variables is determined mostly by a relation N^2 versus number of channels (S, S^2 or A depending on the considered case). While the corresponding comparison in terms of number of constraints is based on a relation N^4 versus number of links L multiplied by number of channels (S, S^2 or A). Therefore, if the number of channels used in the modelling significantly exceeds N^2, the channel-based model experiences higher complexity than the slice-based model.

TABLE II

COMPLEXITY OF SLICE-BASED ILP FORMULATIONS (N=NUMBER OF NODES, W=NUMBER OF WAVELENGTHS OF THE WDM GRID, H=NUMBER OF TRANSCEIVER'S BAUD RATES)

	Fixed Grid Fx/Mf		Flexi Grid Fx/Mf		Fixed Grid Br/Mf-Br		Flexi Grid Br/Mf-Br	
Setting	Var.	Constr.	Var.	Constr.	Var.	Constr.	Var.	Constr.
RSA	$\propto 2N^2(W+2)$	$\propto N^2(2W+5)$	$\propto 4N^4$	$\propto 10N^4$	$\propto 2N^2(W+H+1)$	$\propto N^2(2W+5)$	$\propto 4N^4$	$\propto 10N^4$
RSA-R	$\propto 2N^3$	$\propto N^2(2W+5)$	$\propto 4N^4$	$\propto 10N^4$	$\propto 2HN^3$	$\propto N^2(2W+5)$	$\propto 4N^4$	$\propto 10N^4$
RSA-G	$\propto 2N^4$	$\propto N^4$	$\propto 6N^4$	$\propto 13N^4$	$\propto 2N^4$	$\propto N^4$	$\propto 6N^4$	$\propto 13N^4$
RSA-RG	$\propto 2N^4$	$\propto N^4$	$\propto 6N^4$	$\propto 13N^4$	$\propto 2N^4$	$\propto N^4$	$\propto 6N^4$	$\propto 13N^4$

TABLE III

COMPLEXITY OF CHANNEL-BASED ILP FORMULATIONS (N=NUMBER OF NODES, L=NUMBER OF LINKS, S=NUMBER OF SLICES OF THE FLEXIGRID, A=NUMBER OF SPECTRUM CHANNELS, H=NUMBER OF TRANSCEIVER'S BAUD RATES)

	All feasible channels			
	Fixed Grid Fx/Mf		Flexi Grid Fx/Mf	
Setting	Var.	Constr.	Var.	Constr.
RSA	$\propto 2N^2(S+1)$	$\propto 4N^2+LS$	$\propto 2N^2(H+S^2)$	$\propto 4N^2+LS^2$
RSA-R	$\propto 2N^2(S+N)$	$\propto 4N^2+LS$	$\propto 2N^2(HN+S^2)$	$\propto 4N^2+LS^2$
RSA-G	$\propto 2N^2(S^2+N^2)$	$\propto 3N^2+LS^2$	$\propto 2N^2(N^2+S^2)$	$\propto 3N^4+LS^2$
RSA-RG	$\propto 2N^2(S^2+N^2)$	$\propto 3N^2+LS^2$	$\propto 2N^2(N^2+S^2)$	$\propto 3N^4+LS^2$

	Only selected channels			
	Fixed Grid Br/Mf-Br		Flexi Grid Br/Mf-Br	
Setting	Var.	Constr.	Var.	Constr.
RSA	$\propto 2N^2(A+1)$	$\propto 4N^2+LA$	$\propto 2N^2+(H+A)$	$\propto 4N^2+LA$
RSA-R	$\propto 2N^2(A+N)$	$\propto 4N^2+LA$	$\propto 2N^2+(HN+A)$	$\propto 4N^2+LA$
RSA-G	$\propto 2N^2(A+N^2)$	$\propto 3N^2+LA$	$\propto 2N^2+(N^2+A)$	$\propto 3N^4+LA$
RSA-RG	$\propto 2N^2(A+N^2)$	$\propto 3N^2+LA$	$\propto 2N^2+(N^2+A)$	$\propto 3N^4+LA$

VI. RESULTS

We consider a ring topology as described in Section III with $N = 8$ nodes and 500 km radius. The offered traffic is 1-to-all, i.e., one node is elected as gateway and it establishes bidirectional communications with all the other nodes, or all-to-all, meaning that every node communicates to each other node of the ring. The spectrum is divided in frequency slices (FS) of $F = 6.25$ GHz in the flexi grid, and 50 GHz in the fixed case. The total available optical spectrum per link is 1 THz, from which it follows that in the fixed-grid case the total number of wavelength is 20, whereas in the flexigrid case the number of slices is 160. Mf transceivers support dual-polarization QPSK and n-QAM, with $n = 8, 16, 32, 64$. Br transceivers can work at two baud rates ($H_1 = 14$ or $H_2 = 28$ Gbaud, occupying an optical bandwidth of $3F = 18.75$ GHz and $5F = 31.25$ GHz, respectively). The transmission reaches for these transceivers are reported in Table I. In case of superchannel formation, the superchannel bandwidth is computed as an integer multiple of the channel bandwidth of each transceiver. Guardband spacing is $G = F = 6.25$ GHz.

For the flexi grid, we consider the following transceivers: (1) Fx DP-QPSK transceivers operating at 28 Gbaud; (2) Mf transceivers operating at 28 Gbaud; (3) Br DP-QPSK transceivers (either 14 or 28 Gbaud); (4) Br-Mf transceivers. In the fixed grid transceivers can be Fx or Mf, always at 28 Gbaud. The objective function to be minimized is N_t (note that in case of regeneration, we set $\Gamma = 1.2$), and, among the solutions minimizing N_t, we chose the one with minimal S_o.

In Fig. 4 we can see that grooming allows a small reduction of N_t only for low traffic in both fixed and flexi grid (such reduction is even smaller in case of regeneration). Note that, since in the flexi grid the signal reaches are shorter than in the fixed grid (as the ratio e/B is higher), flexi grid requires a slightly larger N_t than fixed grid, especially for high traffic. The advantages of flexi grid emerge if we consider S_o (Fig. 5) that is always significantly reduced using flexi grid. Results with mixed values (14 and 28 Gbaud) of baud rates are not reported as they do not affect the N_t (but a minor gain in terms of S_o can be observed).

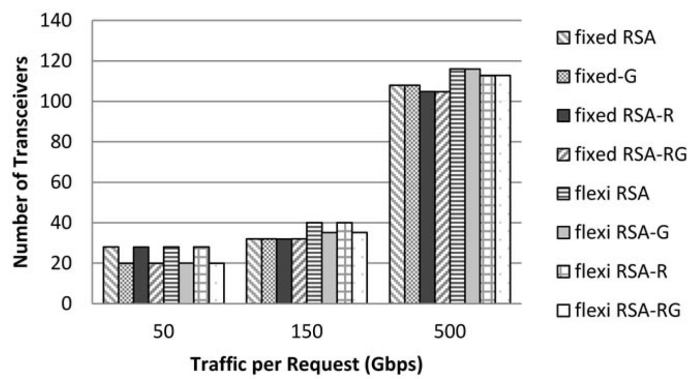

Fig. 4. Transceiver utilization for $R = 500$ km with 28 Gbaud Mf transceiver and 1-to-all traffic matrix, when minimizing N_t. The width of the frequency slices in the flexi grid is $F = 6.25$ GHz.

The computational time required to obtain the optimal solution using the CPLEX solver is plotted in Fig. 6. We can see that introducing traffic grooming has a significant impact for low traffic volumes, where numerous grooming alternatives must be considered, thus dominating the complexity increase due to the flexible grid. Conversely, for higher traffic, grooming capabilities become less useful (as offered traffic easily saturates the transceiver capacity) and the additional complexity due to managing the flexi grid emerges (on average one order of magnitude higher computational times w.r.t. the fixed grid). Finally, note that including variable modulation formats, regeneration and multiple baud rates does not lead to remarkable increases in the computational times (less than one order of magnitude) w.r.t. the benchmark RSA scenario with single QPSK modulation format and 28 Gbaud

TABLE IV

SPECTRUM OCCUPATION, TRANSCEIVER UTILIZATION AND COMPUTATIONAL TIME (ORDER OF MAGNITUDE) FOR $R = 500$ KM WITH 28 GBAUD MF TRANSCEIVERS AND ALL-TO-ALL TRAFFIC MATRIX, WHEN MINIMIZING N_t. THE WIDTH OF THE FREQUENCY SLICES IN THE FLEXI GRID IS $F = 6.25$ GHZ.

Fixed Grid Mf									
Traffic	50 Gb/s			150 Gb/s			500 Gb/s		
Setting	S_o	N_t.	Comput. Time	S_o	N_t.	Comput. Time	S_o	N_t.	Comput. Time
RSA	6400	112	1 s	128	8000	100 ms	-	-	-
RSA-R	6400	112	1 s	128	8000	100 ms	-	-	-
RSA-G	2000	50	1 h	126	6150	100 s	16000	640	100 ms
RSA-RG	2000	50	1 h	126	6150	100 s	16000	536	100 s
Flexi Grid Mf									
Traffic	50 Gb/s			150 Gb/s			500 Gb/s		
Setting	S_o	N_t.	Comput. Time	S_o	N_t.	Comput. Time	S_o	N_t.	Comput. Time
RSA	4800	112	10 s	7300	160	100 s	-	-	-
RSA-R	4800	112	10 s	4800	140.8	1 s	-	-	-
RSA-G	1450	54	10 h	4762	150	10 h	10100	640	10 h
RSA-RG	1450	54	10 h	4800	140.8	10 s	10387.5	536	10 h

TABLE V

SPECTRUM OCCUPATION, TRANSCEIVER UTILIZATION AND COMPUTATIONAL TIME (ORDER OF MAGNITUDE) FOR $R = 500$ KM WITH 28 GBAUD MF TRANSCEIVERS AND 1-TO-ALL TRAFFIC MATRIX, WHEN MINIMIZING S_o. THE WIDTH OF THE FREQUENCY SLICES IN THE FLEXI GRID IS $F = 6.25$ GHZ.

Fixed Grid Mf									
Traffic	50 Gb/s			150 Gb/s			500 Gb/s		
Setting	S_o	N_t.	Comput. Time	S_o	N_t.	Comput. Time	S_o	N_t.	Comput. Time
RSA	1600	28	10 μs	2000	32	10 μs	6600	108	10 μs
RSA-R	1600	28	10 μs	1600	32.8	10 μs	4800	112.8	10 μs
RSA-G	700	20	100 s	1500	36	1 s	4200	168	1 s
RSA-RG	700	20	100 s	1500	36	10 s	4200	168	10 s
Flexi Grid Mf									
Traffic	50 Gb/s			150 Gb/s			500 Gb/s		
Setting	S_o	N_t.	Comput. Time	S_o	N_t.	Comput. Time	S_o	N_t.	Comput. Time
RSA	1200	28	100 μs	1825	44	100 μs	4700	116	100 μs
RSA-R	1200	28	100 μs	1200	35.2	100 μs	3200	112.4	100 μs
RSA-G	506.25	24	100 s	1025	60	1 s	2712.5	168	1 s
RSA-RG	506.25	23.2	$10^3 s$	1025	57.6	10 s	2712.5	168	1 s

TABLE VI

NR. OF TRANSCEIVERS AND COMPUTATIONAL TIME FOR THE EUROPEAN-LIKE NETWORK (ONLY FIXED GRID).

Traffic (Gb/s)	RSA		RSA-R		RSA-G		RSA-RG	
	Transc.	Time (s)	Transc.	Time (s)	Transc.	Time (s)	Transc.	Time (s)
20	55	0.2	55	9.14	16	33698	16	77398
50	55	0.34	55	11.87	26	1179	25.2	51002
100	55	0.34	55	11.54	43	1512	43	36809

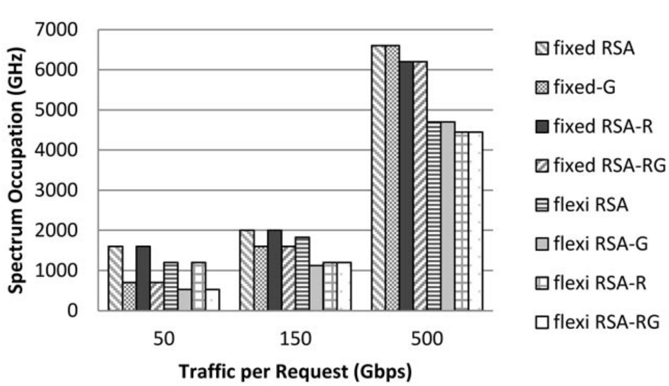

Fig. 5. Spectrum occupation for $R = 500$ km with 28 Gbaud Mf transceiver and 1-to-all traffic matrix, when minimizing N_t. The width of the frequency slices in the flexi grid is $F = 6.25$ GHz.

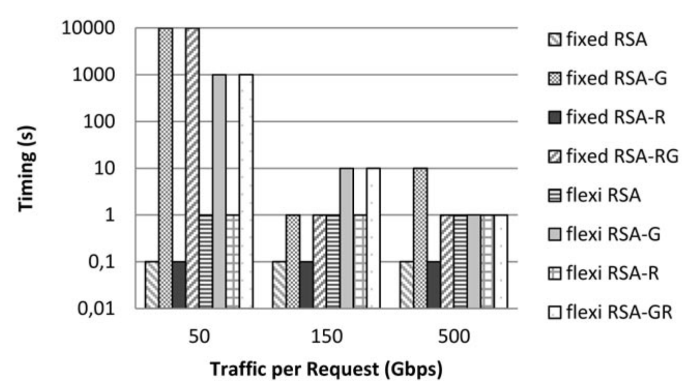

Fig. 6. Computational time (order of magnitude) for $R = 500$ km with 28Gbaud Mf transceivers and 1-to-all traffic matrix, when minimizing N_t. The width of the frequency slices in the flexi grid is $F = 6.25$ GHz.

transceivers. Similar results obtained for an all-to-all traffic matrix are summarized in Table IV. With such traffic matrix, the placement of regenerators is much more frequent in the RSA-R and RSA-RG settings, especially for high bit rates. As for the one-to-all scenario, traffic grooming has the heaviest impact on the problem complexity, which in turn increases the computational time required by the CPLEX solver. Note that in absence of traffic grooming, the spectrum occupancy in case of 500 GBd traffic demands exceeds the overall spectrum availability, thus leading to infeasible network configurations.

Table V summarizes the results obtained for the same scenario, in case the objective function to be minimized is S_o (again, among the solutions minimizing S_o, we chose the one with minimal N_t). With this optimization goal it is worth noting that, when grooming is enabled, large superchannels spanning only one physical link are privileged, since short distances allow for the utilization of higher modulation formats (32-QAM for 28 Gbd transceivers and 64- QAM for 14 GBd transceivers), which ensure high spectrum efficiency. Due to the preference for such network configurations, the order of magnitude of the computational times is generally lower than the transceiver minimization case. The drawback is that multiple short superchannels require the installation of a high number of transceivers.

We expect similar considerations to hold for mesh networks. Some preliminary results are reported in Table VI for a European-like fixed grid mesh network [25] with average link length of 550 km. Mesh networks will be object of a follow-up complexity analysis also in the case of flexi grid.

A. Slice-based model vs. channel-based model

We now compare the channel-based model to the slice-based one, assuming the same 8-nodes ring topology described above. We report results related to two most distant cases: pure RSA with fixed transceiver type (Table VII) and RSA-RG with variable modulation format and baud rate (Table VIII). Performance of both cases is analyzed for two objective functions: transceiver utilization and spectrum occupation. The execution time of CPLEX is limited to 3 hours and therefore not all presented results are optimal. First, we discuss the simpler RSA problem. As we can see in Table VII, both ILP modeling approaches provide the same optimal results in relatively short time. However, the execution time of the channel-based model is about 8 times the one required by the slice-based to find the optimal results. In the case of the RSA-RG model, scalability issues in the channel-based model are even more pronounced. As mentioned in the complexity analysis, in case of grooming, the width of channel for a particular lightpath can be of various size. However, if all possible channels are to be considered, we need to generate up to about S^2 possible channels, where S denotes the number of available spectrum slices. Thus, the size of the model grows significantly and as a consequence CPLEX for the considered cases returns out-of-memory error. Therefore, we decided to limit the slice granularity of the channels and we consider channels having size defined as a multiple of 5 slices (i.e., 5 slices, 10 slices, 15 slices, etc.) and a multiple of 3 slices (3 slices, 6 slices, 9 slices, etc.). This approach significantly reduces the number of candidate channels in the modeling and according to our experiments, only with this approach, the CPLEX is able to return some results. However, we must underline that changing the slice granularity of channels means, that the channel-based model is not optimal in a global sense as the slice-based model is, since this assumption can lead to overprovisioning a channel with more slices than required by the number of transceivers used for this lightpath. In Table VIII, we show the results concerning RSA-RG model. We can easily notice that in terms of transceiver utilization both models provide the same results, even though the channel-based model uses only limited set of possible channels due to fixed slice granularity. The execution time of the channel-based model with 5-slice granularity is comparable to the slice-based model, in 3 of 6 reported cases the channel-based model is even faster. The channel-based model with 3-slice granularity is less efficient in terms of the execution time. Performance of both analyzed ILP models in terms of spectrum utilization varies considerably. First, due to changing the channel granularity, the channel-based model yields worse results and the gap with respect to the slice-based model grows when increasing the channel granularity from 3-slice channels to 5-slice channels. In terms of the execution time the gap is large — the slice-based model provides results in few seconds, while the channel-based model in half of the reported cases cannot find optimal result in 3 hours. The presented results confirm the observations provided above, i.e., when introducing additional constraints (grooming, regeneration, variable modulation format and baud rate) the complexity of the channel-based model increases much faster than the slice-based model, especially when the spectrum utilization is the optimization criterion.

VII. Conclusion

This paper analyzes the complexity trade-offs in the design of optical flexigrid networks supporting electronic traffic grooming, regeneration, modulation format and baud rate assignment. Integer linear programs exploiting two different modeling approaches (slice-based and channel-based) are provided and adapted to multiple network settings. First, we have shown that in presence of traffic grooming the additional complexity due to the flexible grid has a minor impact on problem complexity. Similarly, in all the considered scenarios, regeneration and modulation/baud rate assignment do not relevantly impact on the problem complexity. Then by comparing the channel based and slice based models, the analysis of the model complexity and the results of numerical experiments demonstrate that the slice-based model is more scalable than the channel-based one. The slice-based model generally solves problems faster and requires significantly less memory resources, especially when traffic grooming is applied.

VIII. Acknowledgment

The work of Roza Goscien and Krzysztof Walkowiak was supported by the Polish National Science Centre (NCN) under Grant DEC-2012/07/B/ST7/01215. The work of Massimo Tornatore and Krzysztof Walkowiak was supported by the European Commission under the 7th Framework Programme, Coordination and Support Action, Grant Agreement Number 316097, ENGINE - European research centre of Network intelliGence for INnovation Enhancement (http://engine.pwr.wroc.pl/).

References

[1] International Telecommunication Union, Telecommunication Standardization Sector, “Spectral Grids for WDM Applications: DWDM Frequency Grid,” ITU-T Rec. G.694.1, Feb. 2012, Available at: `http://www.itu.int`

TABLE VII
SLICE-BASED MODEL VS. CHANNEL-BASED MODEL FOR RSA WITH FIXED (FX) TRANSCEIVER TYPE, RING NETWORK WITH 8 NODES AND 1000 KM RADIUS AND ALL-TO-ALL TRAFFIC

		Tranceiver utilization				Spectrum utilization			
		Slice-based model		Channel-based model		Slice-based model		Channel-based model	
Traffic per request (Gb/s)	Frequency slice (GHz)	Result	Time [s]	Result	Time [s]	Result	Time [s]	Result	Time [s]
20	6.25	113	1.32	113	25.49	5600	1.27	5600	25.47
50	6.25	113	1.31	113	25.61	5600	1.29	5600	25.48
100	6.25	129	2.30	129	26.71	6800	2.93	6800	26.71
20	12.5	113	2.41	113	6.55	6400	1.35	6400	6.49
50	12.5	113	2.44	113	6.52	6400	1.32	6400	6.50
100	12.5	129	2.40	129	6.62	7600	2.55	7600	6.62

TABLE VIII
SLICE-BASED MODEL VS. CHANNEL-BASED MODEL FOR RSA-RG WITH VARIABLE MODULATION FORMAT AND BAUD RATE (MF-BR), RING NETWORK WITH 8 NODES AND 500 KM RADIUS, 1-TO-ALL TRAFFIC

		Transceiver utilization						Spectrum occupation (GHz)					
		Slice-based model		Channel-based model granularity 3 slices		Channel-based model granularity 5 slices		Slice-based model		Channel-based model granularity 3 slices		Channel-based model granularity 5 slices	
Traffic per request (Gb/s)	Frequency slice (GHz)	Result	Time [s]	Result	Time [s]	Result	Time [s]	Result	Time [s]	Result	Time [s]	Result	Time [s]
20	6.25	16	21	16	637	16	8	350	5	375	25	500	5
50	6.25	20	184	20	581	20	84	563	5	675*	10805	750	211
100	6.25	27	14	27	11	27	4	825	7	975*	10809	1125*	10804
20	12.5	16	15	16	175	16	64	294	7	356	226	313	26
50	12.5	20	192	20	3615	20	613	494	8	563	2395	594*	10814
100	12.5	27	17	27	33	27	19	738	7	863*	10821	938*	10810
100	12.5	27	17	27	33	27	19	738	7	863*	3h	938*	3h

*Not optimal results

[2] Gerstel, O.; Jinno, M.; Lord, A.; Yoo, S.J.B, "Elastic optical networking: a new dawn for the optical layer?," in *Communications Magazine*, vol.50, no.2, pp. 12–20, Feb. 2012

[3] Christodoulopoulos, K.; Tomkos, I.; Varvarigos, E.A., "Elastic Bandwidth Allocation in Flexible OFDM-Based Optical Networks", in *Journal of Lightwave Technology*, vol. 29, no. 9, pp. 1354-1366, May 2011

[4] Velasco, L.; Klinkowski, M.; Ruiz, M.; Comellas, J., "Modeling the routing and spectrum allocation problem for flexgrid optical networks," in *Photonic Network Communications* , vol.24, no.3, pp.177-186, 2012

[5] Tomkos, I.; Azodolmolky, S.; Sole-Pareta,.; Careglio, D.; Palkopoulou, E., "A Tutorial on the Flexible Optical Networking Paradigm: State of the Art, Trends, and Research Challenges," in *Proceedings of the IEEE*, vol.PP, no.99, pp.1,21, Jun. 2014

[6] Ruiz, M.; Pioro, M.; Zotkiewicz, M.; Klinkowski, M.; and Velasco, L.; "Column Generation Algorithm for RSA Problems in Flexgrid Optical Networks", in *Photonic Network Communications*, vol. 26, no. 2-3, pp. 53-64, Dec. 2013

[7] Klinkowski, M.; and Walkowiak, K.; "Routing and Spectrum Assignment in Spectrum Sliced Elastic Optical Path Network", in *IEEE Communications Letters*, vol. 15, no. 8, pp. 884-886, 2011, Aug. 2011

[8] Wang, Y.; Cao, X.; and Hu, Q.; "Routing and Spectrum Allocation in Spectrum-Sliced Elastic Optical Path Networks, *Proc. IEEE International Conference on Communications (ICC)*, Kyoto, Japan, Jun. 2011

[9] Wang, Y.; Cao, X.; Pan, Y., "A Study of the Routing and Spectrum Allocation in Spectrum-sliced Elastic Optical Path Networks," *P*roc. of INFOCOM, Shangai, China, Apr. 2011

[10] Cai, A; Shen, G.; Peng, L; and Zukerman, M.; "Novel Node-Arc Model and Multiiteration Heuristics for Static Routing and Spectrum Assignment in Elastic Optical Networks", in *Journal of Lightwave Technology* 31 (21), 3402-3413, Nov. 2013

[11] Patel, A.; Philip, N.; Ji, N.; Jue, J.P.; Wang, T.; "Routing, wavelength assignment, and spectrum allocation algorithms in transparent flexible optical WDM networks", in *Optical Switching and Networking*, Vol. 9, Issue 3, July 2012, Pages 191-204.

[12] Vizcaino, J.L.; Ye, Y.; Lopez, V.; Jimenez, F.; Musumeci, F.; Tornatore, M.; Pattavina, A.; and Krummrich, P.M.; Protection in optical transport networks with fixed and flexible grid: Cost and energy efficiency evaluation, in *Optical Switching and Networking*, Volume 11, Part A, January 2014, Pages 55-71

[13] Zhang, M.; Lu, W.; Zhu Z.; Yin Y., "Planning and provisioning of elastic O-OFDM networks with fragmentation-aware routing and spectrum assignment (RSA) algorithms," *P*roc. Communications and Photonics Conference (ACP), Guangzhou, China, Nov. 2012

[14] Shirazipourazad, S.; Chenyang Zhou; Derakhshandeh, Z.; Sen, A., "On routing and spectrum allocation in spectrum-sliced optical networks," in *INFOCOM*, Turin, Italy, Apr. 2013

[15] Talebi, S; Bampis, E.; Lucarelli, G.; Katib, Y.; and Rouskas, G.N.; "On Routing and Spectrum Assignment in Rings", Submitted for publication

[16] Popescu, I.; Cerutti, I.; Sambo, N.; Castoldi, P., "On the optimal design of a spectrum-switched optical network with multiple modulation formats and rates," in *IEEE/OSA Journal of Optical Communications and Networking*, vol.5, no.11, pp.1275,1284, Nov. 2013

[17] Zotkiewicz, M.; Pioro, M.; Ruiz, M.; Klinkowski, M.; Velasco, L., "Optimization models for flexgrid elastic optical networks," in *ICTON*, Cartagena, Spain, Jun. 2013

[18] Chen, B. ; Xie, W.; Zhang, J.; Jue, J. P., Zhao, Y. ; Huang, S.; and Gu, W.; "Energy and Spectrum Efficiency with Multi-Flow Transponders and Elastic Regenerators in Survivable Flexible Bandwidth Virtual Optical Networks," in *Optical Fiber Communication Conference,* San Francisco (CA), USA, 2014.

[19] Zami, T., "Co-optimizing Allocation of Nyquist Superchannels and Physical Impairments Aware Placement of Regenerators in Elastic WDM Networks", in *Journal of Lightwave Technology*, vol.PP, no.99, pp.1,1

[20] Klinkowski, M.; Ruiz, M.; Velasco, L.; Careglio, D.; Lopez, V.; Comellas, J., "Elastic Spectrum Allocation for Time-Varying Traffic in FlexGrid Optical Networks," in *IEEE Journal on Selected Areas in Communications*, Vol.31, No.1, pp.26,38, January 2013

[21] Bosco, G.; Curri, V.; Carena, A.; Poggiolini, P.; Forghieri, F., "On the Performance of Nyquist-WDM Terabit Superchannels Based

on PM-BPSK, PM-QPSK, PM-8QAM or PM-16QAM Subcarriers", in *Journal of Lightwave Technology*, vol.29, no.1, pp.53,61, Jan. 2011

[22] Rottondi, C.; Tornatore, M.; Gavioli, G., "Optical Ring Metro Networks With Flexible Grid And Distance-Adaptive Optical Coherent Transceivers," *Bell Labs Technical Journal* vol.18, no.3, pp.95,110, Dec. 2013

[23] Rottondi, C.; Tornatore, M.; Pattavina, A.; Gavioli, G., "Routing, modulation level, and spectrum assignment in optical metro ring networks using elastic transceivers," *IEEE/OSA Journal of Optical Communications and Networking* , vol.5, no.4, pp.305,315, April 2013

[24] Dutta, R.; and Rouskas, G.; "On Optimal Traffic Grooming in WDM Rings", in *IEEE Journal on Selected Areas in Communications*, Vol. 20, No. 1, pp. 110-121, Jan. 2002.

[25] Rizzelli, G.; Morea, A.; Tornatore, M.; Pattavina, A., "Reach-related Energy Consumption Energy Consumption in IP-over-WDM 100G Translucent Networks", in *Journal of Lightwave Technology*, Vol. 31, No. 11, pp. 1828-1834, June 2013